Prospects of argon as buffer gas in the stopping cell at SHIPTRAP

Anton Roth

Lund University, Sweden, antonrothus@gmail.com

In the SHIPTRAP experiments, at GSI, precise mass measurements of the heaviest nuclei are performed. The SHIPTRAP research group currently holds the world record with direct mass spectrometry on ^{256}Lr. To be able to measure the first superheavy nucleus, it is necessary to improve the efficiency of the entire set-up. The gas stopping cell is essential as it concerns the efficiency. In this report the prospects of changing the buffer gas from helium to argon is evaluated.

1 Introduction - Mass measurements of the heaviest nuclei

The main goal of the Penning trap mass spectrometer SHIPTRAP is to perform precise mass measurements on exotic heavy nuclei. The set-up is located behind the velocity filter SHIP, Separator for Heavy Ion reaction Products. The heavy elements are created in a fusion evaporation reaction. Here, the fusion of typically a lighter projectile with a heavier target is followed by an evaporation of neutrons. SHIP separates out the "slow" reaction products from the "fast" primary beam by their velocity with a symmetric composition of dipole magnets and dipole electrical fields [1].

The transmitted heavy ions from SHIP typically have kinetic energies of several 10 MeV. To be able to trap the ions in the subsequent penning trap system, it is necessary to slow them down to a few eV, otherwise they would just fly through the trapping potential. Therefore, the ions are decelerated in a thin foil of titanium before they interact with an inert gas, classically helium, in the gas stopping cell. The stopped ions are then extracted from the cell using a combination of electric fields and a gas jet, before they are guided to the mass measurement set-up. The mass measurements at SHIPTRAP are performed with a penning trap based system. A superconducting magnet confines the trapped ions in the radial direction and the ions are axially confined in a quadrupole electric field. In the trap the ions perform a circular motion with a frequency characteristic to their mass. Through different techniques the characteristic frequency can be measured very

precise and the mass of the ion can be determined with a high precision [1].

SHIPTRAP holds the world record of direct mass measurement of the heaviest nucleus, ^{256}Lr ($Z = 103$). The combination of significantly lower production cross sections and steadily shorter half-lives for even heavier nuclei, presents a challenge for the SHIPTRAP set-up. Towards the first mass measurement of a superheavy element, *i.e.* $Z \geq 104$, an improvement on the set-up efficiency, and especially that of the gas stopping cell, is crucial [2, 1].

The efficiency of the gas cell is governed by the fraction of ions which are stopped within the geometry of the cell, denoted as stopping efficiency, and the fraction of ions that are stopped which then are extracted from the gas cell, denoted as extraction efficiency. A new, more efficient cell, denoted as CryoCell, has been under development since 2008 and its first online commissioning was conducted in 2015 [3]. The combined stopping and extraction efficiency is anticipated to approach 70 % [2].

With the current Ti-foil thickness a significant fraction of the ions already come to a stop in the entrance window and are lost [4]. Therefore, a thinner foil is desired, which in turn requires either a larger helium pressure or a buffer gas with larger stopping power to obtain a better stopping efficiency. The pressure with helium is limited, but argon represents a buffer gas with a larger stopping power.

In the following, the prospects of argon as the stopping cell buffer gas at SHIPTRAP is evaluated, based on the experimental settings of the 2015 online commissioning experiment. After a description of the CryoCell, simulations of the stopping efficiency with argon using the

program SRIM are discussed. Here, simulation settings; the choice of ion and the energy and spatial distributions of the incoming ion are examined, followed by a discussion on the simulation results. Finally, the benefits and limitations for the usage of argon are concluded and an outlook for future prospects is given.

2 The CryoCell, the gas stopping cell at SHIPTRAP

The CryoCell, schematically drawn in Fig. 1, is a gas cell cooled to cryogenic temperatures to improve the purity of the gas. The basic principle of the cell is that the high energy recoils from SHIP lose a fraction of their kinetic energy in the entrance window, made of titanium, and are completely stopped in the cell after collisions with a buffer gas. With an electrostatic field gradient created by the so called DC-cage, a cylindrical structure composed of 8 ring electrodes, the stopped ions are guided further to the Radio Frequency funnel (RF-funnel). The RF-funnel also consists of ring electrodes but here the ring radii decreases and the funnel hence resembles a conical shape. A DC-gradient generated with the ring electrodes drags the ions towards the extraction nozzle. Additionally, in the RF-funnel a 180º phase shifted radio frequency between the neighbouring ring electrodes is applied. The AC-field induces a force on the ions perpendicular to the surface of the funnel and therefore focuses the ions towards the extraction nozzle. Here, the gas flow towards the vacuum section behind the nozzle transports the ions further to the penning trap system. In
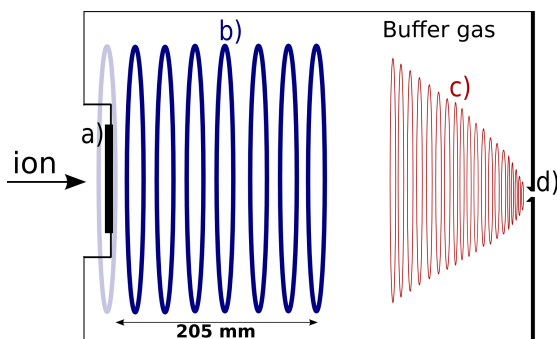

Fig. 1: *Sketch of the CryoCell. The arrow indicates the direction of the ions from SHIP. The Ti-foil entrance window is labelled a), the DC-cage b), the RF-funnel c) and the extraction nozzle d). For details the reader is referred to section 2.*

order to extract the ions from the CryoCell it is crucial to avoid any charge exchange resulting in a neutralisation. This is why an inert noble gas such as helium is used. The heavy ions can also be lost due to molecule formation. To minimise the risk of neutralisation the cell is cooled down to 40 K, at which the residual gas molecules, such as water, are not gaseous and will freeze out on any surface of the gas cell [2].

In this context, the noble gas argon is an alternative buffer gas. The stopping power of argon is larger compared to helium enabling thinner entrance windows which is foreseen in future. A higher pressure would be required with helium to stop the ions within the cell. An increased helium pressure requires a larger amplitude on the funnel RF-voltage to maintain the focusing towards the extraction nozzle. But at larger voltages discharges have been observed which ruin the purity of the helium gas and result in a decreased efficiency. By exchanging helium with argon, as suggested in Ref. [4], the probability of discharge might be lowered. With a larger stopping power and a lowered discharge probability, argon as the buffer gas can potentially increase the efficiency of the CryoCell.

3 Simulation settings

3.1 Choice of ion

The simulations are performed in SRIM, Stopping and Range of Ions in Matter. The highest Z number available in SRIM is 92, uranium. Hence, to be able to simulate ^{254}No ($Z = 102$) it is necessary to choose an ion with properties such that it resembles the supposed behaviour of nobelium in the energy region and material of interest. Extrapolation models to the stopping power of ^{254}No [5, 6] and the quality of the SRIM stopping power were thoroughly studied for titanium. Due to similar stopping power values of the extrapolated models and that of SRIM for ^{238}U, ^{238}U was chosen as the ion with no energy modification.

3.2 Initial recoil energy distribution

^{254}No is created in the fusion evaporation reaction ^{208}Pb(^{48}Ca, $2n$)^{254}No at a beam energy of 4.55 MeV/A. In the 2015 online commissioning the target was composed of three layers. The first layer, facing the beam, consisted of carbon (C) and the second of a mixture of lead (Pb),

sulfur (S) and tin (Sn). A thin carbon layer was added to the back of the PbSSn-layer. Further target details, such as densities and the thickness (mg/cm^2) of the different elements in the layers were taken from Ref. [4].

The ^{48}Ca-ions lose energy in the first C-layer and in the PbSSn-layer till the fusion reaction occurs. The created ^{256}No* are deexcited through an instantaneous isotropic evaporation of 2n and the ^{254}No-ions lose energy in the remaining part of the PbSSn-layer and the subsequent C-layer. As the fraction of energy which is lost in the target is small, a constant stopping power across the target is a good approximation. Measured stopping power values of ^{48}Ca and a modelled stopping power of ^{254}No for the different elements were used [4]. The stopping power of the ions in the mixed PbSSn-layer was computed as the sum of the individual element stopping powers multiplied with the element abundance in the layer.

With the assumption that the fusion can take place anywhere in the PbSSn-layer a uniform kinetic energy distribution of the ^{254}No after the target is obtained extending from 33.2 ± 1.2 to 38.2 ± 0.2 MeV. Here the uncertainties origin from a varied thickness of the PbSSn layer which is motivated by large fluctuations in the manufactured target.

A normalised velocity distribution has been measured after SHIP of the reaction of interest [1]. A Gaussian velocity distribution of the ^{254}No-ions before entering the gas cell was measured. The measured Gaussian distribution was transformed into a kinetic energy distribution and was superposed on the uniform $[33.2 \pm 1.2, 38.2 \pm 0.2]$ MeV distribution. The edges of the normalised measured velocity distribution was chosen as $[32, 38.5]$ MeV. The resulting distribution, presented in Fig. 2, was used as the initial kinetic energy of the ^{254}No ions entering the CryoCell in the SRIM simulations.

3.3 Initial recoil spatial distribution

The ^{254}No-ions entering the gas cell feature a spatial distribution. The ion beam spot has been measured to 50×30 mm and the entrance window of the CryoCell is circular with a diameter of 60 mm [2]. In the SRIM simulation an initial spatial distribution with the shape of a 2D-Gaussian distribution was assumed. The widths $FWHM_x, FWHM_y$ were taken from the
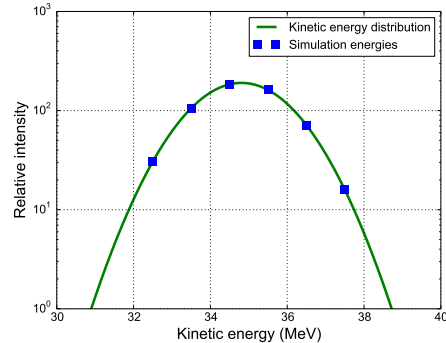

Fig. 2: *Initial kinetic energy distribution (filled green line) of the ^{254}No-ions. The blue squares indicate the input energies used in the SRIM simulation.*

measured beam shape after SHIP on the online experiment 2015 [4] and the centres of gravity μ_x, μ_y were simply assumed as the centre of the window.

4 Results - Simulated stopping efficiencies

First, the implementations of a specific initial energy and initial spatial distribution, compared to previous work in Ref. [4], were investigated. In the former study a helium buffer gas was used and therefore the comparisons are made to a helium buffer gas at the optimal pressure of 50 mbar. A first evaluation showed that the
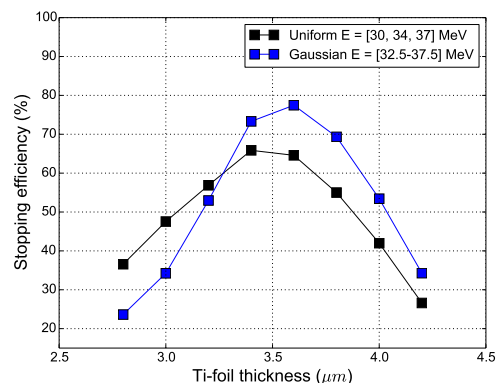

Fig. 3: *Effect on the stopping efficiency of the initial energy distribution. The Gaussian energy distribution in this work (see section 3.2) and the uniform energy distribution based on [30,34,37] MeV in Ref. [4] is presented in black and blue, respectively.*

stopping efficiency was not influenced by a spatial distribution of the ions entering the gas cell.

The small spatial distribution compared to the gas cell dimensions is most likely the reason for this. A spatial distribution was therefore neglected in the continued analysis. The effect on the stopping efficiency for a different initial energy distribution is presented in Fig. 3. With the initial recoil energy distribution used in this work it is evident that the stopping efficiency maximum is increased and the stopping efficiency peak occurs at a slightly larger Ti-foil thickness when compared to the uniform distribution employed in Ref. [4].

The main result of this work concerns the stopping efficiency of argon in the CryoCell. The stopping efficiency for different argon pressures and 50 mbar helium is presented in Fig. 4. It is very difficult to manufacture Ti-foils with a thickness $< 3.2\,\mu$m. With this in mind and that the extraction efficiency increases with larger pressures, 12.5 mbar seems to be a sufficient argon pressure. From Fig. 4, it is also clear that it is possible to accomplish a significantly larger stopping efficiency of 90 % with 12.5 mbar of argon, compared to an efficiency of 77 % with 50 mbar of helium.

tribution which reflected experimental measurements was also included in the simulation. Compared to former investigations this increased the stopping efficiency and extended the stopping efficiency maximum towards a larger foil thickness. With argon it is possible to gain a stopping efficiency from 50 mbar with $3.6\,\mu$m Ti-foil thickness of 77 % to 90 % of 12.5 mbar argon with a $3.2\,\mu$m Ti-foil thickness. Hence, from the aspect of the stopping efficiency it is advantageous to use argon instead of helium for a future superheavy element experiment. For experiments of lighter nuclei, $e.g.$ in the $N = Z$ region, the kinetic energies of the recoils are larger. The larger stopping power of argon can really come to use and significantly increase the stopping efficiency of the CryoCell for such experiments.

The efficiency of the CryoCell is governed by the combined stopping and extraction efficiency. The extraction efficiency with argon as a stopping cell buffer gas deserves further investigations and experimental measurements to determine its usefulness.
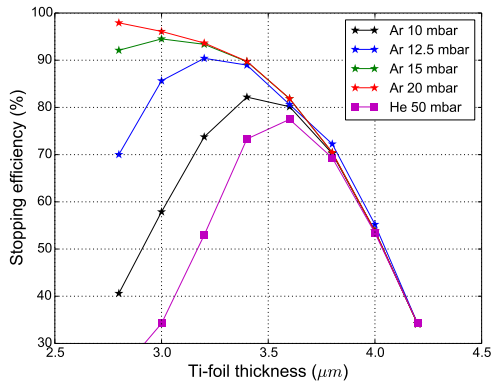
Acknowledgements

Fig. 4: *The stopping efficiency as a function of the Ti-foil thickness for different argon pressures and 50 mbar helium as indicated in the legend.*

5 Conclusions and future prospects with argon as a buffer gas

The stopping efficiency of the CryoCell with argon as a buffer gas has been simulated. To the simulation a spatial distribution was implemented which had a negligible effect on the stopping efficiency. An initial kinetic energy dis-

References

[1] M. G. Dworschak (2014) (Doctoral dissertation).

[2] C. Droese *et. al. Nucl. Instr. and Meth.* B **338**, (2014) 126-138.

[3] O. Kaleja *et. al.* (2015) (GSI Scientific Report).

[4] O. Kaleja (2016) (Master thesis).

[5] L. C. Northcliffe and R. F. Schilling. *Nuclear Data Tables*, A7, 233-463 (1970).

[6] D. Wittwer *et. al. Nucl. Instr. and Meth.* B **268** (2010) 2835.